

Investigations on Structural and luminescence of Anatase/Rutile Titania Stimulated RE³⁺ ions

G.Subalakshmi^{a*}, R. Thilagaraj Benisha^a, K.Theerthi^a, S.Santhiya^a

^aDepartment of Physics, Theivanai Ammal College for Women, Villupuram-605401

Abstract

The present paper reports infrared emission from upconversion luminescence spectra of RE³⁺ doped TiO₂ phosphor. Sample was prepared by precipitation method at variable doping concentration of ytterbium using TiCl₄ as a raw material. Their structure, band gap energy and luminescence properties are investigated using X-ray diffraction, diffuse reflectance spectroscopy, and photoluminescence spectroscopy. The photoluminescence spectra recorded under the 330 nm excitation with the variable concentration of ytterbium. The PL emission spectra shows intense emission peaks near infrared regions.

Keywords : Precipitation method, RE³⁺, PL, X-ray diffraction

Introduction

Solar energy deems much attention to overcome the global energy crisis being a renewable, pollution free and abundant source of energy in the universe [1]. Solar cells are used to convert the solar energy to electricity, Si-based solar cells in particular predominate the solar cell market due to the 15% conversion efficiency [2]. The spectral discrepancy in the c-Si solar cell is the principal reason for major energy loss [3].

Downshifting- converting high energy photons into lower energy photons is much recommended technique to modify spectrum, enhancing the efficiency of Si-based solar cells thereby minimize the energy loss [4]. Luminescent industries widely use rare earth ions in 4f states, completely filled 5S² and 5S⁶ orbital for emitting wide range luminescence from ultraviolet to NIR region [5]. Yb³⁺, known for possessing only two energy levels, ²F_{5/2} and ²F_{7/2} is much consistent for string NIR emission around 1000 nm betwixt the transition level, therefore Yb³⁺ in the NIR region is the maximum spectral response of the c-Si solar cell [6].

The host material chosen determines the down-conversion luminescence property. Of late doping semiconducting compounds with RE ions either to control or tune the optical property utilizing unique band gap structure has proven successful [7]. Due to its good thermal, chemical and mechanical properties TiO₂ is taken for study to assess the NIR emission intensity [8,9]. The method synthesis, purity and presence of dopants defines the optical property of TiO₂ which may alter the impact if found wanting [10,11]. Of varies methods developed for the synthesis of TiO₂ nanoparticles, flame synthesis[12], ultrasonic irradiation [13], chemical vapour deposition [14], sol-gel process [15], hydrothermal [16], solvothermal [17], and precipitation [18], the last method simple, effective.

In this study, study the performance of mixed Anatase and Rutile titania properties. The structure formation, luminescence properties and energy transfer mechanism are discussed in detail.

Material and methods

The TiO₂:xYb³⁺ ions at different compositions (x = 0.03, 0.06, 0.09, 0.12) is prepared by precipitation method. TiCl₄, Yb₂O₃, H₂SO₄ and ammonia solution are used in the experiments without any further purification. Fresh distilled water is used for making aqueous solution. In precipitation process, 10 ml of TiCl₄ is dissolved in 100 ml of ice-cold deionized H₂O followed by constant and steady stirring overnight to obtain the solution. Yb₂O₃ solution (Yb₂O₃ dissolved in the sulfuric acid) is added to the host solution and stirred well. Then mixed solution is added drop by drop to ammonia solution which is used as the precipitation agent. Once the precipitate settles

at the bottom of the flask, it is filtered and washed with several times with distilled water. The washed precipitate is dried by muffle furnace for 24 hours. Finally, the obtained material is calcined for 4 hours at 600°C in Muffle furnace and allowed to cool naturally.

The X-ray diffraction pattern (XRD) is obtained on a D8 advance X-ray diffractometer (Bruker) equipment using Cu-K α ($\lambda = 1.54065 \text{ \AA}$) radiation to identify the structure and phase purity. The XRD patterns of the sample are collected at 2θ , between 20° and 60°. The Varian Model 5000 UV-Vis spectrophotometer is used to

measure the absorbance spectrum of the samples different doping concentration. The Photoluminescence emission spectra are recorded using Spectrofluorometer (JY Fluorolog-FL3-11). The excitation and emission measurement are effected by 450W Xenon lamp. All measurements are recorded at room temperature.

Results and discussion

The diffraction pattern gives an idea about the crystallinity and phase structure of the synthesis sample. Fig.1 shows the diffraction patterns of ytterbium doped titania compound. From this analysis, it is clear that the sample annealed at 600°C shows diffraction peaks implies the presence of anatase and rutile phase which well match with the JCPDS data of Card No. 076173 & 89-4920. Present composition suppresses the intensity of the rutile phase (110) peak aggravates the intensity of anatase phase revealing the mixed phase of TiO₂ [19]. The relative propositions of anatase and rutile can be evaluated using spurr equation [20]

$$F_R = \frac{1}{1+8[I_A(101)+I_R(110)]} \times 100 \quad (1)$$

Where, F_R is the mass fraction of rutile, and $I_A(101)$ and $I_R(110)$ are the intensities of anatase and rutile peaks,

respectively. From the calculation, it is noted the percentage of the rutile phase is 30.89, 36.93 and 21.80.

UV-Visible reflectance spectrum is focused in order to characterize the optical absorbance of the TiO₂ doped ytterbium ions (Fig.2).The absorption spectrum of the doping samples is show a shift towards blue region as compared to the pure TiO₂. Although the spin transition originates from Yb³⁺:²F_{5/2} to ²F_{7/2} the absorption peaks around ~1000 nm. The reflectance data were converted into absorption ones using the Kubelka-Munk transformation according to Equation

$$F(R) = (1-R) / 2R$$

The band gap energy for each sample was estimated by the Tauc's law described

$$F(R)=\alpha h\nu = A (h\nu - E_g)^n \quad (2)$$

Where α is absorption coefficient, h represents the Planck's constant, ν denotes the frequency of light, A is the characteristic parameter for transition, E_g is the band gap value and n is a constant depending on the nature of the electron transition ($n= 2$ for direct transition or $1/2$ for indirect transition). The indirect band gap is plotted for $(\alpha h\nu)^{1/2}$ versus photon energy ($h\nu$) (Fig. 3). The indirect band gap energy of present compound is 2.89eV, 3 eV, 3.01eV,3.02 and 3.04eV.

The photoluminescence spectrum of the synthesis materials at different doping concentrations ($x = 0.03, 0.06, 0.09$ and 0.12) is shown in Fig.4. The excitation at 330 nm and near NIR emission intensity at 982, 997, 1026, 1055nm wavelength and intense emission is observed at 1026 nm. The doping concentration of Yb³⁺ varying at 0.03 to 0.12. Peak position of PL spectrum shows significant steep at 1026 nm due to the varying concentration of ytterbium ions. Despite several weak peaks due to transition at different stark level ²F_J ($J=5/2, 7/2$), the intensity of emission from the TiO₂:xYb³⁺ at 1026 nm is relatively higher than the band edge of c-silicon solar cell.

The energy transfer mechanism of the host material to Yb³⁺ ions is explain in the schematic energy levels diagram in Fig.5. First, the material is excited under ultraviolet (UV) region at 330 nm and the electron transition

takes place from the valence band to the conduction band in TiO₂ compound. This causes intense emission around NIR region due to the ET process of Yb³⁺ ions for, Yb³⁺ ions have two electronic states namely ²F_{7/2} and ²F_{5/2} and the energy transfer occurs between ²F_{7/2} and ²F_{5/2}. The two energy states splits into seven stark levels, 1 to 4 levels for the ground ²F_{5/2} and 5-7 levels for ²F_{7/2} excited state. The intense peak at 1026 nm attributed to the transition from stark the peaks at lower wavelength 982, 997 and 1055 nm and are due to transition 5 → 1, 2, 3 and 4 transition states respectively. The concentration of the ytterbium ions is place a pivotal role on the increasing the emission intensity.

Micro electronics industry development relies much on c-Si based solar cell due to its abundance, high energy conversion efficiency and economy [23]. Yet the c-Si solar cells suffer major drawback of spectral loss due to low efficiency output caused by thermalization of hot carrier. To recap this loss, the down-conversion material is used to increase photocurrent generation. The sample down-conversion material (TiO₂:Yb³⁺) equates the c-Si bases solar cell in the spectral region around 1000 nm. Thus the down-conversion material taken for the study conform efficiency enhancement of c-Si solar cell.

Conclusion

The sum up, TiO₂:Yb³⁺ is synthesized by precipitation method and its phase structure, luminescence properties and energy transfer mechanism are discussed in detail. Posing against different doping concentration of ytterbium ions recorded to be the concentration registering efficient emission in NIR region. Excited at 330 nm formation of several weak peaks may distract concentration level that the intensity formed at 1026 nm ensures the characteristic emission of ²F_{5/2} → ²F_{7/2} electronic state transition of Yb³⁺ ions. The TiO₂:Yb³⁺ NIR material is authenticated for a solar spectral converter development and is adept for c-Si solar cell devices.

Acknowledgment

The authors gratefully acknowledge the the SAIF of IIT, Madras for PXRD, Pondicherry University for DRS-UV and PL study.

References

- [1] Luciano de A. Florêncio, Luis A. Gómez-Malagón, Bismarck C. Lima, Anderson S.L. Gomes, J.A.M Garcia, Luciana R.P. Kassab, Efficiency enhancement in solar cells using photon down-conversion in Tb/Yb- doped tellurite glass, *Solar Energy Materials & Solar Cells* 157 (2016) 468–475.
- [2] Bo Fan, Christophe Chlique, Odile Merdrignac-Conanec, Xianghua Zhang, Xianping Fan, Near-Infrared Quantum Cutting Material Er³⁺/Yb³⁺ Doped La₂O₂S with an External Quantum Yield Higher than 100%, *J. Phys. Chem. C* 116 (2012) 11652–11657.
- [3] A. Boccolini, J. Marques-Hueso, D. Chen, Y. Wang, B.S. Richards, Physical performance limitations of luminescent down-conversion layers for photovoltaic applications, *Solar Energy Materials & Solar Cells* 122 (2014) 8–14.
- [4] Mark B. Spitzer, Hans P. Jenssen, Arlete Cassanho, An approach to downconversion solar cells, *Solar Energy Materials & Solar Cells* 108 (2013) 241–245.
- [5] B.S. Richards, Luminescent layers for enhanced silicon solar cell performance: Down-conversion, *Solar Energy Materials & Solar Cells*, 90 (2006) 1189-1207.
- [6] L. de S. Menezes, G. S. Maciel, Cid B. de Araújo, Y. Messaddeq, Phonon-assisted cooperative energy transfer and frequency upconversion in a Yb³⁺/Tb³⁺ codoped fluorindate glass, *J. Appl. Phys.* 94 (2003) 863-866.
- [7] Ji-Guang Li, Xiaohui Wang, Kenji Watanabe, Takamasa Ishigaki, Phase Structure and Luminescence Properties of Eu³⁺-Doped TiO₂ Nanocrystals Synthesized by Ar/O₂ Radio Frequency Thermal Plasma Oxidation of Liquid Precursor Mists, *J. Phys. Chem. B* 110 (2006) 1121-1127.
- [8] M.M. Rahman, K.M. Krishna, T. Soga, T. Jimbo, M. Umeno, Optical properties and X-ray photoelectron spectroscopic study of pure and Pb-doped TiO₂ thin films, *Journal of Physics and Chemistry of Solids* 60 (1999) 201–210.

- [9] Nadica D. Abazovic, Mirjana I. Comor, Miroslav D. Dramićanin, Dragana J. Jovanovic S. Phillip Ahrenkiel, Jovan M. Nedeljkovic, Photoluminescence of Anatase and Rutile TiO₂ Particles, *J. Phys. Chem. B* 110 (2006) 25366-25370.
- [10] D. Reyes-Coronado, G. Rodríguez-Gattorno, M.E. Espinosa-Pesqueira, C. Cab, R. de Coss, G. Oskam, Phase-pure TiO₂ nanoparticles: anatase, brookite and rutile, *Nanotechnology* 19 (2008) 145605(10pp).
- [11] J. Arbiol, J. Cerda, G. Dezanneau, A. Cirera, F. Peiro, A. Cornet, J. R. Morante, Effects of Nb doping on the TiO₂ anatase-to-rutile phase transition, *J. Appl. Phys.* 92 (2002) 853-861.
- [12] Kranthi K. Akurati, Andri Vital, Roland Hany, Bastian Bommer, Thomas Graule, Markus Winterer, One-step flame synthesis of SnO₂/TiO₂ composite nanoparticles for photocatalytic applications, *International journal of Photoenergy* 7 (2005) 153-161.
- [13] Jimmy C. Yu, Jianguo Yu, Wingkei Ho, Lizhi Zhang, Preparation of highly photocatalytic active nano-sized TiO₂ particles *via* ultrasonic irradiation, *Chem. Commun.*(2001) 1942–1943.
- [14] Mitsutaka Okumura, Shyunichi Nakamura, Susumu Tsubota, Toshiko Nakamura, Masashi Azuma, Masatake Haruta, Chemical vapor deposition of gold on Al₂O₃, SiO₂, and TiO₂ for the oxidation of CO and of H₂, *Catalysis Letters* 51 (1998) 53–58.
- [15] Jeffrey C.-S. Wu, Chih-Hsien Chen, A visible-light response vanadium-doped titania nanocatalyst by sol-gel method, *Journal of Photochemistry and Photobiology A: Chemistry* 163 (2004) 509–515.
- [16] Jiefang Zhu, Wei Zheng, Bin He, Jinlong Zhang, Masakazu Anpo, Characterization of Fe–TiO₂ photocatalysts synthesized by hydrothermal method and their photocatalytic reactivity for photodegradation of XRG dye diluted in water, *Journal of Molecular Catalysis A: Chemical* 216 (2004) 35–43.
- [17] Sang-Hyeun Lee, Misook Kang, Sung M. Cho, Gui Young Han, Byung-Woo Kim, Ki June Yoon, Chan-Hwa Chung, Synthesis of TiO₂ photocatalyst thin film by solvothermal method with a small amount of water and its photocatalytic performance, *Journal of Photochemistry and Photobiology A: Chemistry* 146 (2001) 121–128.
- [18] Hee-Dong NAM, Byung-Ha LEE, Sun Jae KIM, Chung-Hwan JUNG, Ju-Hyeon LEE, Sung PARK, Preparation of Ultrafine Crystalline TiO₂ Powders from Aqueous TiCl₄ Solution by Precipitation, *Jpn.J.Appl.Phys.* 37 (1998) 4603-4608.
- [19] Maria Suzana P. Francisco, Valmor R. Mastelaro, Inhibition of the Anatase-Rutile Phase Transformation with Addition of CeO₂ to CuO-TiO₂ System: Raman Spectroscopy, X-ray Diffraction, and Textural Studies, *Chem. Mater.* 14 (2002) 2514-2518.
- [20] P. Prasannalakshmi, N. Shanmugam, N. Kannadasan, K. Sathishkumar, G. Viruthagiri, R. Poonguzhali, Influence of thermal annealing on the photocatalytic properties of TiO₂ nanoparticles under solar irradiation, *J. Mater. Sci: Mater. Electron.* 26 (2015) 7987.
- [21] Hai Guo, Ning Dong, Min Yin, Weiping Zhang, Liren Lou, Shangda Xia, Visible Upconversion in Rare Earth Ion-Doped Gd₂O₃ Nanocrystals, *J. Phys. Chem. B* 108 (2004) 19205-19209.
- [22] K. Karthik, S. Dhanuskodi, C. Gobinath, S. Sivaramkrishnan, Microwave-assisted synthesis of CdO–ZnO nanocomposite and its antibacterial activity against human pathogens, *Spectrochimica Acta Part A: Molecular and Biomolecular Spectroscopy* 139 (2015) 7–12.
- [23] Jozef Szlufcik, S. Sivarthaman, Johan F. Nijs, Robert P. Mertens, Roger Van Overstraeten, Low-Cost Industrial Technologies of Crystalline Silicon Solar Cells, *Proceedings of the IEEE*, 85 (1997) 711-730.

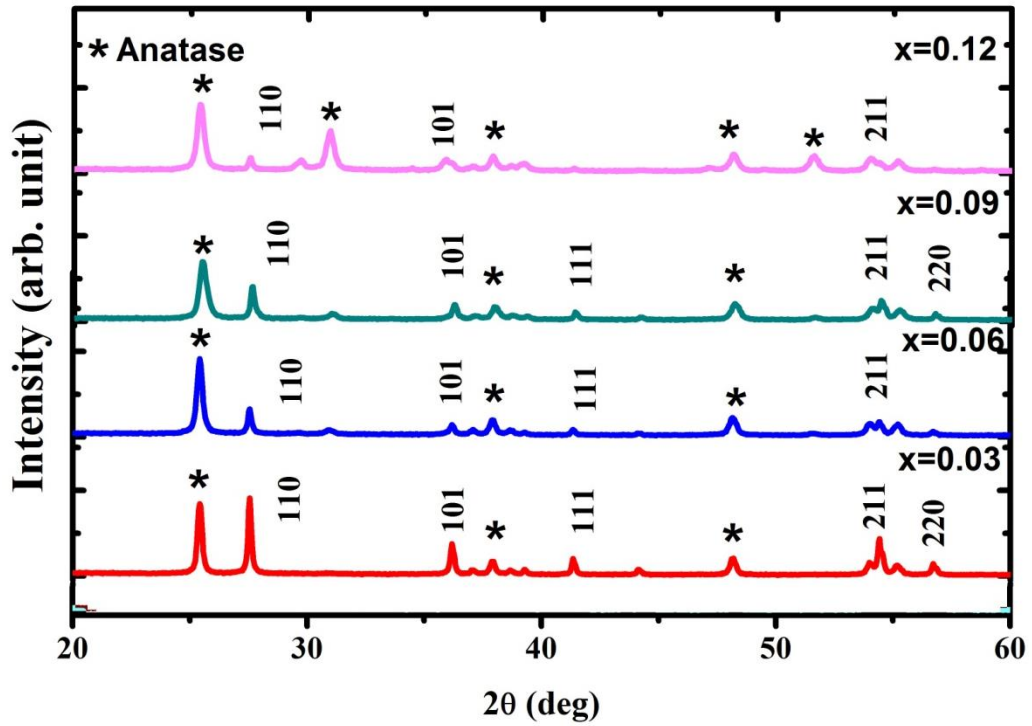


Fig. 1

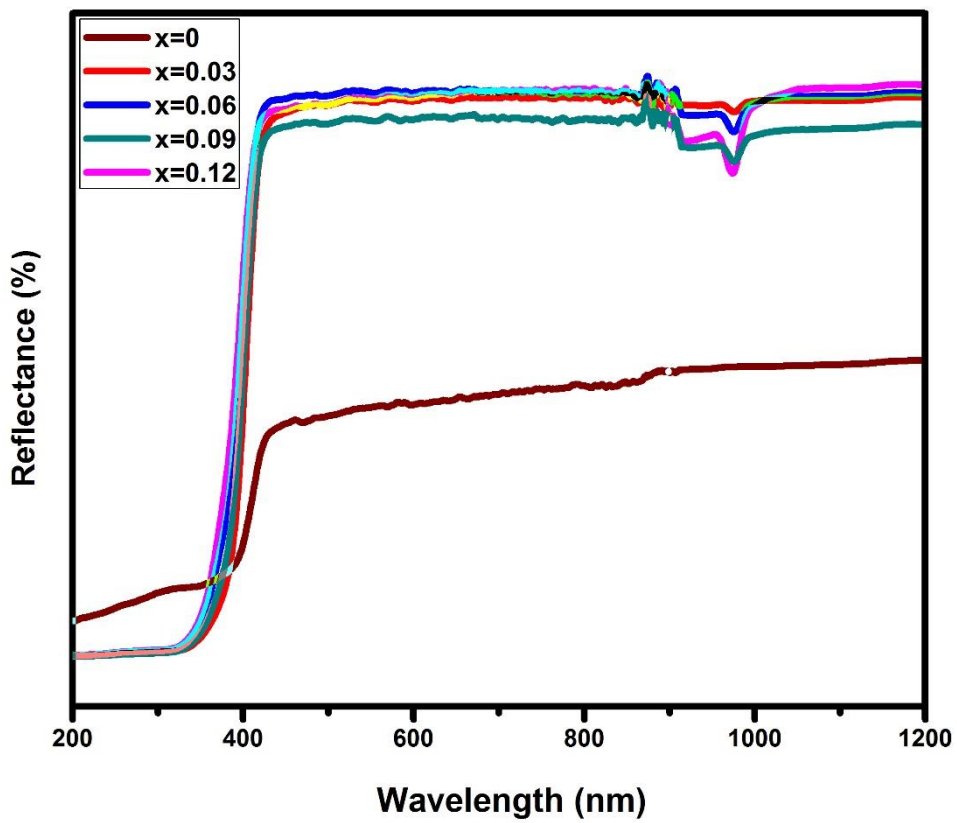


Fig. 2

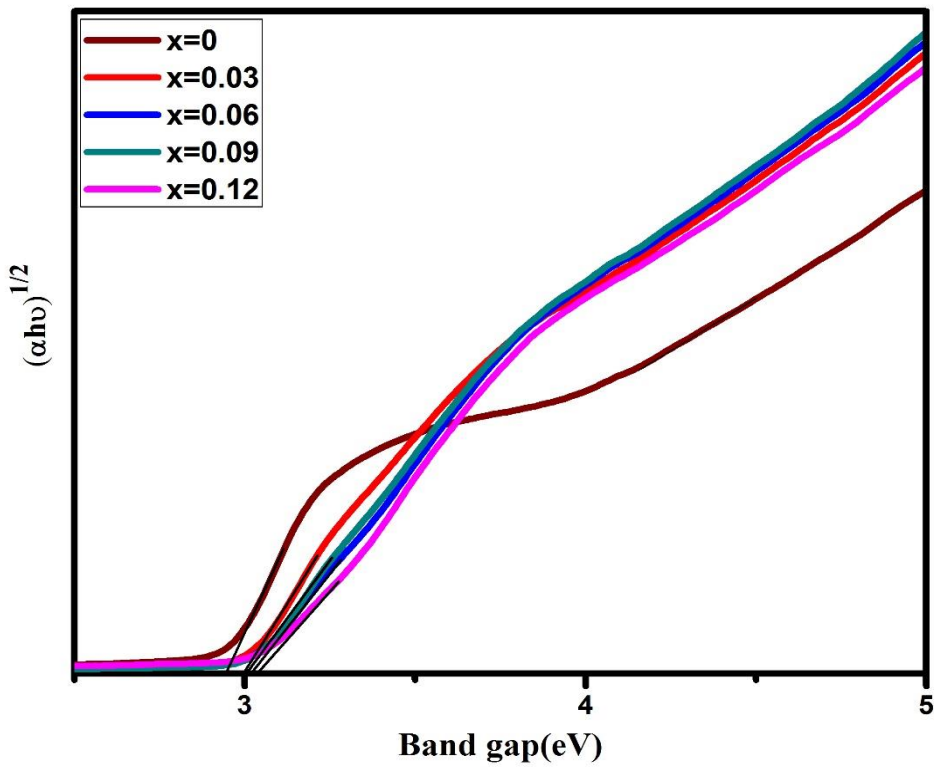


Fig. 3

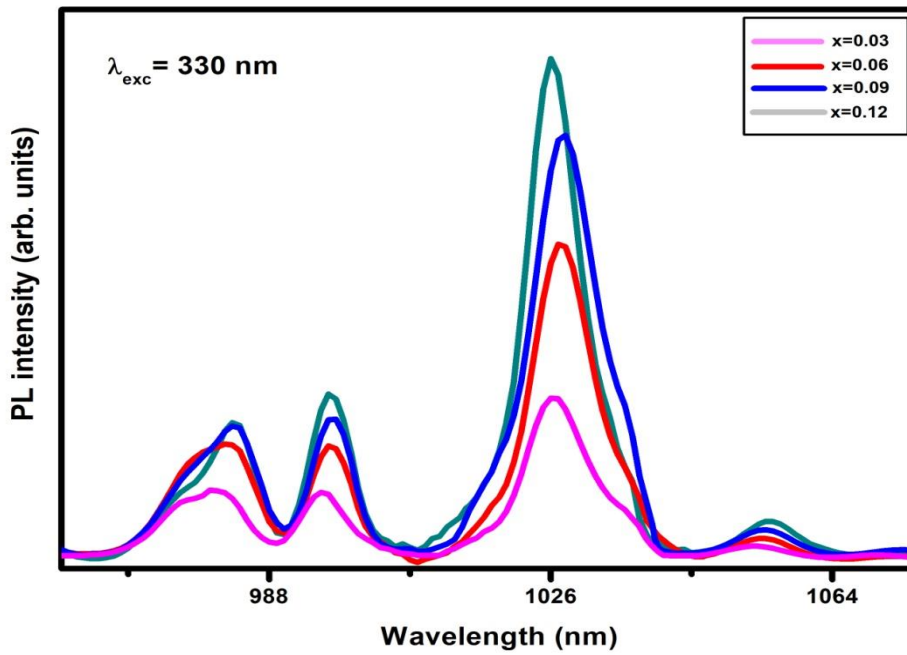


Fig. 4

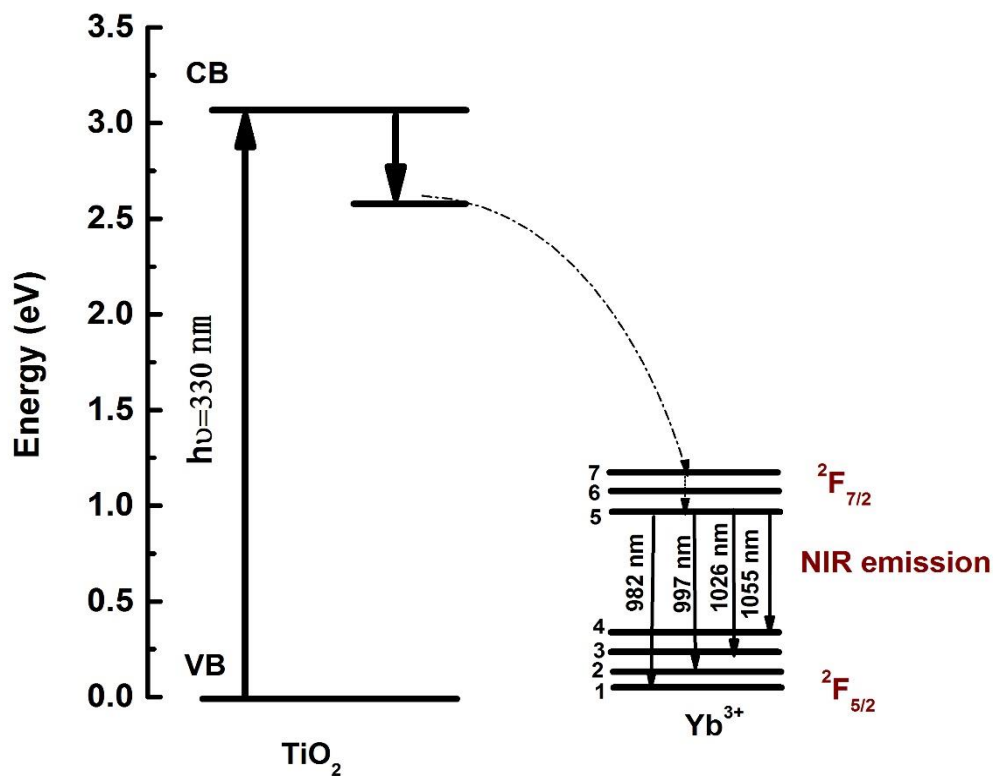


Fig. 5

Figure caption

- Fig. 1** X ray diffraction of rutile phase TiO_2 and Yb^{3+} doped TiO_2 phosphor ($x=0.03$ to 0.12)
- Fig. 2** Diffuse reflectance spectrum of rutile phase TiO_2 and Yb^{3+} doped TiO_2 phosphor ($x=0.03$ to 0.12)
- Fig. 3** Indirect band gap energy rutile phase TiO_2 and Yb^{3+} doped TiO_2 phosphor ($x=0.03$ to 0.12)
- Fig. 4** photoluminescence emission spectrum of Yb^{3+} doped TiO_2 phosphor ($x= 0.03, 0.06, 0.09$ and 0.12)
- Fig. 5** Energy level diagram of ytterbium doped TiO_2